AD-A081 467 AVCO SYSTEMS DIV WILMINGTON MA F/G 20/13
HYPERSONIC HEAT TRANSFER TEST PROGRAM IN THE VKI LONGSHOT FACIL--ETC(U)
DEC 79 V DICRISTINA F49620-79-C-0013
UNCLASSIFIED AVSD-0335-79-CR AFOSR-TR-80-0124 NL

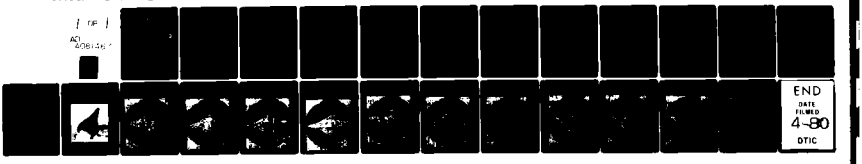

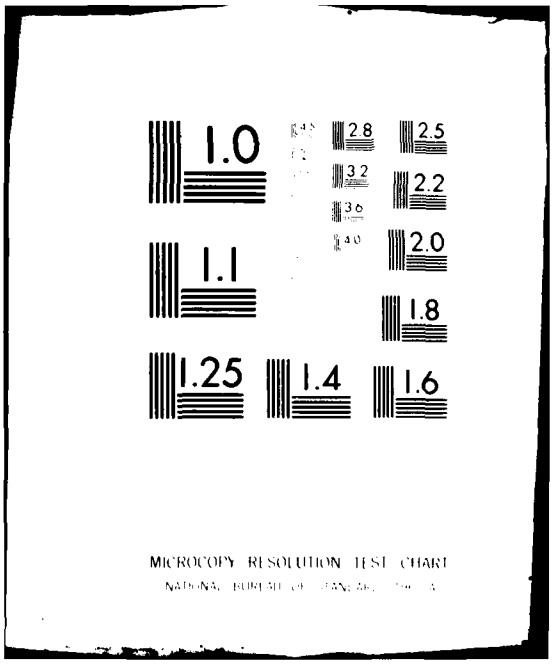
1.0
1.1
1.25
1.4
1.6
1.8
2.0
2.2
2.5
2.8
3.2
3.6
4.0
MICROCOPY RESOLUTION TEST CHART

HYPERSONIC HEAT TRANSFER TEST PROGRAM IN THE VKI LONGSHOT FACILITY

Test Summary Report

18 December 1979

AVSD-0335-79-CR
K500-79-VD-32

Contract No. F49620-79-C-0013

Prepared for

Department of the Air Force
Air Force Office of Scientific Research (AFSC)
Bolling Air Force Base, D. C. 20332

AVCO SYSTEMS DIVISION
201 LOWELL ST. WILMINGTON, MASS.

UNCLASSIFIED

SECURITY CLASSIFICATION OF THIS PAGE (When Data Entered)

REPORT DOCUMENTATION PAGE

READ INSTRUCTIONS BEFORE COMPLETING FORM

1. REPORT NUMBER: AFOSR-TR-80-0124	2. GOVT ACCESSION NO.
3. RECIPIENT'S CATALOG NUMBER	
4. TITLE (and Subtitle): HYPERSONIC HEAT TRANSFER TEST PROGRAM IN THE VKI LONGSHOT FACILITY.	5. TYPE OF REPORT & PERIOD COVERED: FINAL, 01 Dec 78-30 Nov 79
6. PERFORMING ORG. REPORT NUMBER: AVSD-0335-79-CR	
7. AUTHOR(s): VICTOR DICRISTINA	8. CONTRACT OR GRANT NUMBER(s): F49620-79-C-0013
9. PERFORMING ORGANIZATION NAME AND ADDRESS: AVCO CORPORATION/AVCO SYSTEMS DIVISION, 201 LOWELL STREET, WILMINGTON, MASSACHUSETTS 01887	10. PROGRAM ELEMENT, PROJECT, TASK AREA & WORK UNIT NUMBERS: 61102F, 2307A1
11. CONTROLLING OFFICE NAME AND ADDRESS: AIR FORCE OFFICE OF SCIENTIFIC RESEARCH/NA, BLDG 410, BOLLING AIR FORCE BASE, D C 20332	12. REPORT DATE: 18 DECEMBER 1979
	13. NUMBER OF PAGES: 25
14. MONITORING AGENCY NAME & ADDRESS (if different from Controlling Office)	15. SECURITY CLASS. (of this report): UNCLASSIFIED
	15a. DECLASSIFICATION/DOWNGRADING SCHEDULE

16. DISTRIBUTION STATEMENT (of this Report)

Approved for public release; distribution unlimited

17. DISTRIBUTION STATEMENT (of the abstract entered in Block 20, if different from Report)

18. SUPPLEMENTARY NOTES

19. KEY WORDS (Continue on reverse side if necessary and identify by block number)

HYPERSONIC FLOW
BICONIC
REENTRY VEHICLE
HEAT TRANSFER

20. ABSTRACT (Continue on reverse side if necessary and identify by block number)

A summary of test results is presented for local pressure and heat transfer distributions on a biconic body for a range of hypersonic Mach numbers, Reynolds number, and angle-of-attack. The model configuration approximated nosetip contours typical of low altitude turbulent ablated shapes. Instrumentation included a longitudinal row of ten pressure taps and, 180 degrees apart, a row of eleven smooth calorimeter discs. The tests were performed in the Longshot Facility of the von Karman Institute for Fluid Dynamics.

404 744

DD FORM 1 JAN 73 1473 EDITION OF 1 NOV 65 IS OBSOLETE

UNCLASSIFIED

3

HYPERSONIC HEAT TRANSFER TEST PROGRAM

IN THE VKI LONGSHOT FACILITY

Test Summary Report

18 December 1979

AVSD-0335-79-CR
K500-79-VD-32

Contract No. F49620-79-C-0013

Prepared for

Department of the Air Force
Air Force Office of Scientific Research (AFSC)
Bolling Air Force Base, D. C. 20332

AVCO SYSTEMS DIVISION
201 LOWELL ST., WILMINGTON, MASS.

TABLE OF CONTENTS

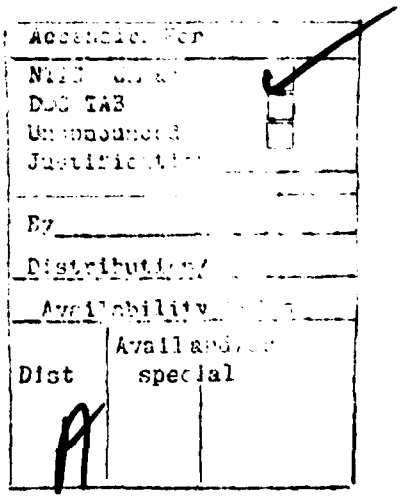

1.0 INTRODUCTION AND SUMMARY

A series of tests was performed in the Longshot Facility of the Von Karman Institute for Fluid Dynamics (VKI) in Rhode-St-Genese, Belgium, in support of USAF Great AFOSR 78-3474. This post-test report is a summary of sixteen tests conducted in the Longshot Facility during the period of 5-15 June 1979 (Phase I) and 3-14 September 1979 (Phase II). The complete test results are included in the VKI post-test report to be published under separate cover.

The purpose of these tests was to measure local pressure and heat transfer distributions on a biconic body configuration over a range of Mach number, Reynolds number and angle-of-attack conditions.

The calorimeter instrumentation was calibrated at VKI during the period 2-4 May 1979. The instrumented test model was delivered to the VKI facility for the first series of tests on 5 June 1979. Surface data measurements were made as planned including schlieren photographs of the model bow shock structure.

2.0 DISCUSSION

2.1 Test Facility

The VKI Longshot facility was used for this program. Longshot differs from a conventional gun tunnel in that a heavy piston is used to compress the nitrogen test gas to very high pressure and temperatures. The test gas is then trapped in a reservoir at peak conditions by the closing of a system of check values. The flow conditions decay monotonically during 20 milliseconds running time as the nitrogen trapped in the reservoir flows through the 6^{o} half angle conical nozzle into the pre-evacuated open jet test chamber. The maximum supply conditions used in these tests are approximately 60,000 lb/in^2 at $1900^{o}K$ to $2350^{o}K$. These conditions provide nominally unit Reynolds numbers of 8.5×10^6 per foot at a Mach number of 16 and 3.5×10^6 at M = 20.

2.2 Model Design

The test model design was a biconic body configuration shown in Figure 1. This model configuration, designated as model N,

approximates nosetip contours typical of low altitude turbulent ablated shapes. The model was fabricated of 303 stainless steel having a wall thickness of approximately 0.2 inches. The model was designed in two segments as shown to facilitate instrumentation gage installation. Figure 2 shows the assembled test model.

2.3 Instrumentation

The test model was instrumental with both pressure and heat flux gages. The gage locations are shown in Figure 1. The test model contains eleven heat flux gages and ten pressure taps. Only nine pressure measurement channels were available at the test facility. The last pressure tape near the base on the model was not connected. PCB model 112A21 high resolution pressure transducers were connected through short flexible tubes to the surface taps.

The heat transfer gages are smooth calorimeter discs fabricated from .004 inch high conductivity copper stock. A 1 mil wire chromel alumel thermocouple is welded to the copper disc which is bonded to an insulating holder. Twenty-four calorimeters were fabricated and calibrated at the VKI facility. Table I lists the measured calibration constant (C_T) for each gage. The values shown are the average of two measurements. The actual measured disc thickness (X_A) is also shown compared with the calculated effective disc thickness (XE). The data was derived from the following relationships:

$$C_T = \frac{\dot{Q}_C}{\Delta E / \Delta t}$$

$$X_E = \frac{C_T}{\rho C_P} = .00523\ C_T$$

where

$\dot{Q}_C$ = calibration heat flux
$\Delta E / \Delta t$ = thermocouple EMF output
X_E = effective gage thickness
C_T = calibration constant
ρ = density, copper
C_P = specific heat, copper

The difference between the actual and effective gage thickness is due to the thermocouple weld joints.

2.4 Test Matrix

The matrix for the sixteen runs made in the Phase I and II test series is shown in Table II. The pressure and heat transfer gages are 180 degrees apart as shown in Figure 1. In order to obtain a complete distribution of pressure and heat transfer measurements for the angle-of-attack cases, both a positive and negative incidence angle was run for the same test conditions as shown in Table II.

2.5 Test Results

The data measurements for each run included schlieren photos of the model flow field in the windward and leeward planes. Figures 3 to 13 show the bow shock and flow field structure for each case.

The measured surface pressure and heat transfer distribution are shown in Tables III and IV, respectively. Problems with the nosetip instrumentation (gage 0) precluded measurement of the stagnation point heat flux. Predictions of the stagnation point heating for each Mach No.-Reynolds No. condition at zero angle of attack is included in Table IV. It should be noted that for a positive angle of attack the heat transfer gages are in the windward position and the pressure gages in the leeward position and vice versa for the negative angles of attack.

TABLE I

Heat Transfer Gage Calibration Data

Gage No.	Avg. Calib. Coeff., C_T	Effect. Gage Thickness, X_E (in.)	Actual Gage Thickness (in.)
1	0.624	.0033	.0038
2	1.235	.0065	.0037
3	0.628	.0033	.0036
5	0.607	.0032	.0040
6	0.658	.0034	.0040
7	0.609	.0032	.0040
8	1.020	.0053	.0040
9	0.654	.0034	.0038
10	0.689	.0036	.0040
12	0.590	.0031	.0039
13	0.934	.0049	.0040
14	0.636	.0033	.0038
15	0.820	.0043	.0036
16	0.598	.0031	.0038
17	1.261	.0066	.0040
18	1.060	.0055	.0039
21	0.669	.0035	.0040
22	--	--	.0040
23	0.625	.0033	.0040
24	0.677	.0035	.0040

TABLE II

VKI Longshot Test Matrix

	Sequence No.	Test Run No.	Model Config.	Angle of Attack (degree)	M_∞	$Re_\infty (ft^{-1})$
PHASE I	1	609	N	0	20	2.0×10^6
	2	610	N	0	20	3.3×10^6
	3	611	N	0	16	4.5×10^6
	4	612	N	0	16	8.6×10^6
	5	616	N	+ 5	20	3.3×10^6
	6	615	N	- 5	20	3.3×10^6
	7	613	N	+ 5	16	8.6×10^6
	8	614	N	- 5	16	8.6×10^6
PHASE II	9	618	N	+20	20	2.0×10^6
	10	624	N	-20	20	2.0×10^6
	11	617	N	+20	20	3.3×10^6
	12	623	N	-20	20	3.3×10^6
	13	619	N	+20	16	4.5×10^6
	14	622	N	-20	16	4.5×10^6
	15	620	N	+20	16	8.6×10^6
	16	621	N	-20	16	8.6×10^6

TABLE III

Surface Pressure Measurements (PSIA)

M	$R_e \times 10^{-6}$ (ft^{-1})	Incid. (deg.)	Run No.	Pitot Pressure (Pt_2)	Gage Location								
					1	2	3	4	5	6	7	8	9
16	9.0	0	612	31.4	1.39	1.31	1.22	1.72	4.45	13.5	6.23	6.11	6.30
		- 5	613	29.6	2.16	2.29	2.51	2.95	14.8	10.3	8.6	8.3	12.5
		+ 5	614	30.2	1.03	0.91	0.86	1.05	1.25	2.31	4.91	7.26	5.32
		-20	620	27.8	8.56	8.84	9.09	8.36	21.5	15.1	13.6	13.7	13.4
		+20	621	30.0	0.44	0.53	0.35	0.38	0.89	0.74	0.54	0.48	--
15	4.5	0	611	16.9	0.96	0.62	0.86	1.48	2.38	6.61	2.95	3.86	4.67
		-20	619	16.2	5.28	5.66	5.57	5.28	14.3	10.34	9.19	9.32	10.6
		+20	622	15.9	0.29	0.33	0.22	0.25	0.55	0.47	0.43	0.30	--
20	3.3	0	610	7.2	0.49	0.47	0.76	0.80	0.96	2.91	2.88	1.65	2.18
		- 5	616	8.3	0.82	0.76	0.88	0.68	5.3	2.8	2.65	2.54	3.04
		+ 5	615	7.71	0.38	0.38	0.58	0.63	0.76	1.08	1.28	1.65	1.8-3.0
		-20	617	7.7	2.82	2.95	2.88	2.73	6.73	4.65	4.22	4.31	4.80
		+20	623	7.32	0.21	0.20	0.16	0.14	0.26	0.20	0.17	0.17	--
20	2.0	0	609	5.44	0.34	0.395	0.54	0.56	0.63	1.57	2.05	1.61	1.34
		-20	618	4.88	2.00	1.89	1.87	1.96	4.78	3.21	3.22	3.25	6.93
		+20	624	4.88	0.11	0.125	0.099	0.915	0.16	0.135	0.138	0.122	-

TABLE IV

Surface Heat Transfer Measurements (Btu/ft^2-sec)

M	$R_e \times 10^{-6}$ (ft^{-1})	Incid. (deg.)	Run No.	Stag. Pt.	Gage Location 1	2	3	4	5	6	7	8	9	10
16	9.0	0	612	(300)*	17.1	9.4	9.8	5.0	40.3	115.8	60.6	-	68.0	72.9
		+ 5	614		22.7	23.5	21.9	21.0	107.7	78.0	129.7	114.3	61.9	80.7
		- 5	613		7.9	7.1	5.6	0	12.9	25.6	57.4	93.1	48.0	45.7
		+20	621		116.8	105.7	155.5	137.4	101.6	70.9	167.5	190.8	140.7	126.2
		-20	620		3.34	3.31	4.10	4.86	16.7	9.1	6.6	5.2	3.2	4.7
15	4.5	0	611	(226)	10.6	13.7	6.5	6.4	20.4	78.6	54.6	65.9	51.8	58.5
		+20	622		55.4	49.4	69.1	76.0	66.3	59.4	107.7	124.9	94.7	79.2
		-20	619		2.69	2.31	3.9	5.30	17.2	7.9	5.5	4.7	4.2	6.7
20	3.3	0	610	(205)	10.8	8.3	4.4	4.1	-	36.8	135.9	41.3	45.4	32.5
		+ 5	615		41.0	33.7	43.2	36.3	95.6	64.2	60.2	82.5	75.8	73.1
		- 5	616		23.4	22.7	14.2	11.8	-	21.0	48.8	72.9	54.2	56.8
		+20	623		62.1	58.1	58.0	33.9	51.9	36.6	76.0	91.0	64.8	58.3
		-20	617		2.7	2.5	3.1	3.8	11.2	8.7	7.0	10.0	6.1	8.5
20	2.0	0	600	(174)	9.3	8.7	4.0	2.9	7.3	12.9	29.0	18.6	21.8	19.9
		+20	624		43.7	41.3	37.5	29.3	36.6	27.3	60.7	90.0	41.9	43.4
		-20	618		1.72	1.31	1.44	1.45	9.86	4.24	4.81	4.51	3.44	4.0

*Predictions

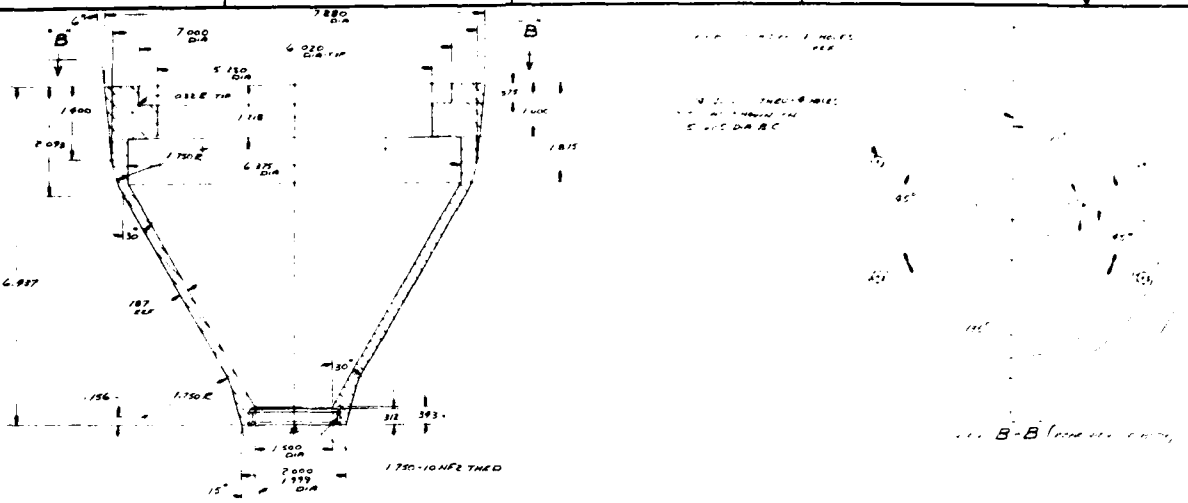

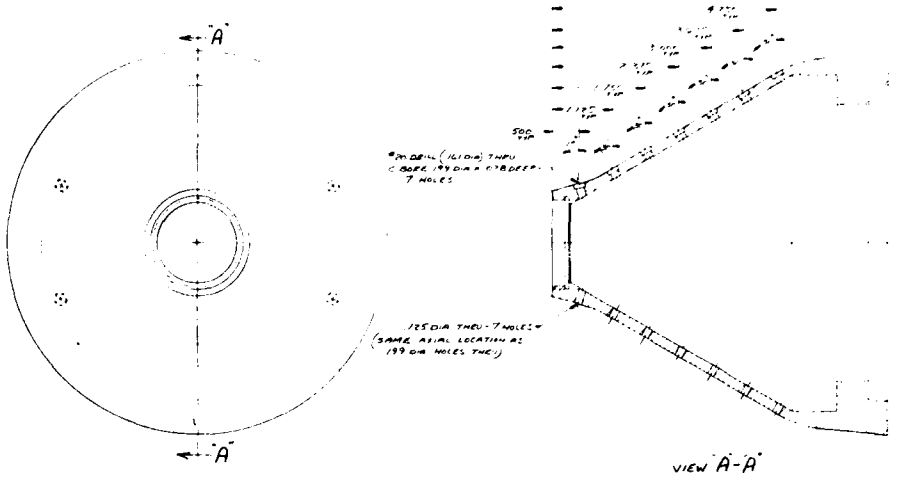

(2) BODY - 1 REQ'D
MAT'L - STN STL 303

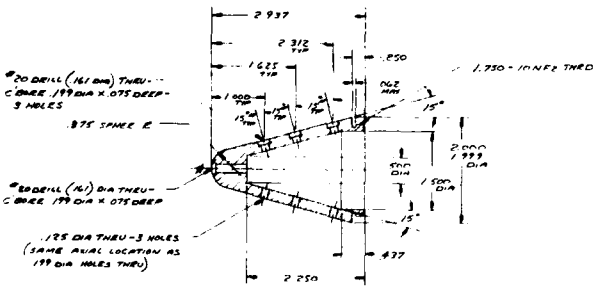

(1) NOSE TIP - 1 REQ'D
MAT'L - STN STL 303

NOTE: ALL HOLES TO BE IN AXIAL ALIGNMENT WITH HOLES IN PART #2 (BODY)

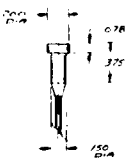

(3) HEAT FLUX GAUGE ASSY - 11 REQ'D
VENDOR: BOLT, BERANEK & NEWMAN CAMBRIDGE, MASS

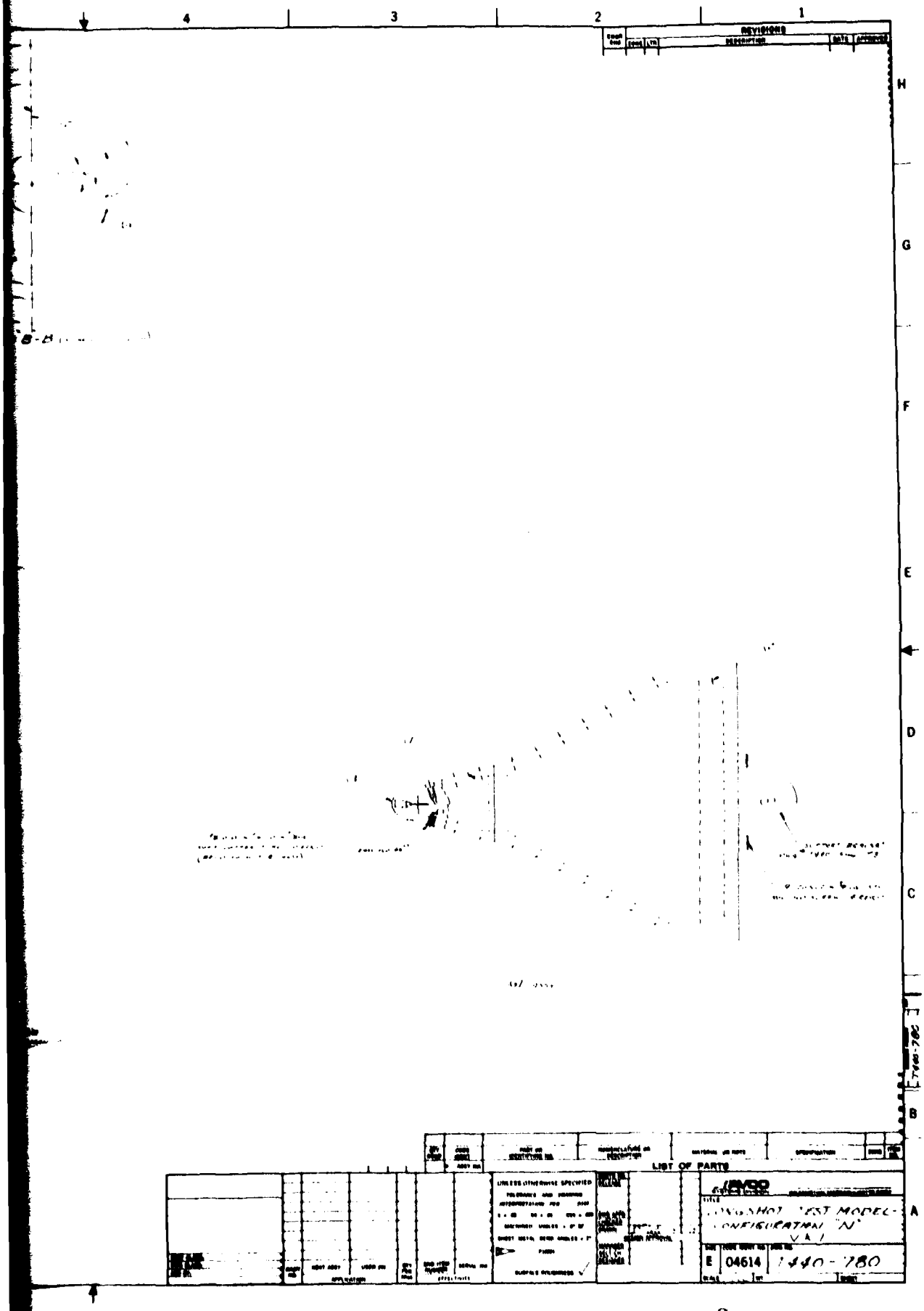

FIGURE 1

FIGURE 2

Assembled Biconic Test Model

FIGURE 3

Schlieren Flow Field
Run No. 609 - Model N
$M_\infty = 20$, $Re_\infty = 2.0 \times 10^6/ft$, $\alpha = 0^\circ$

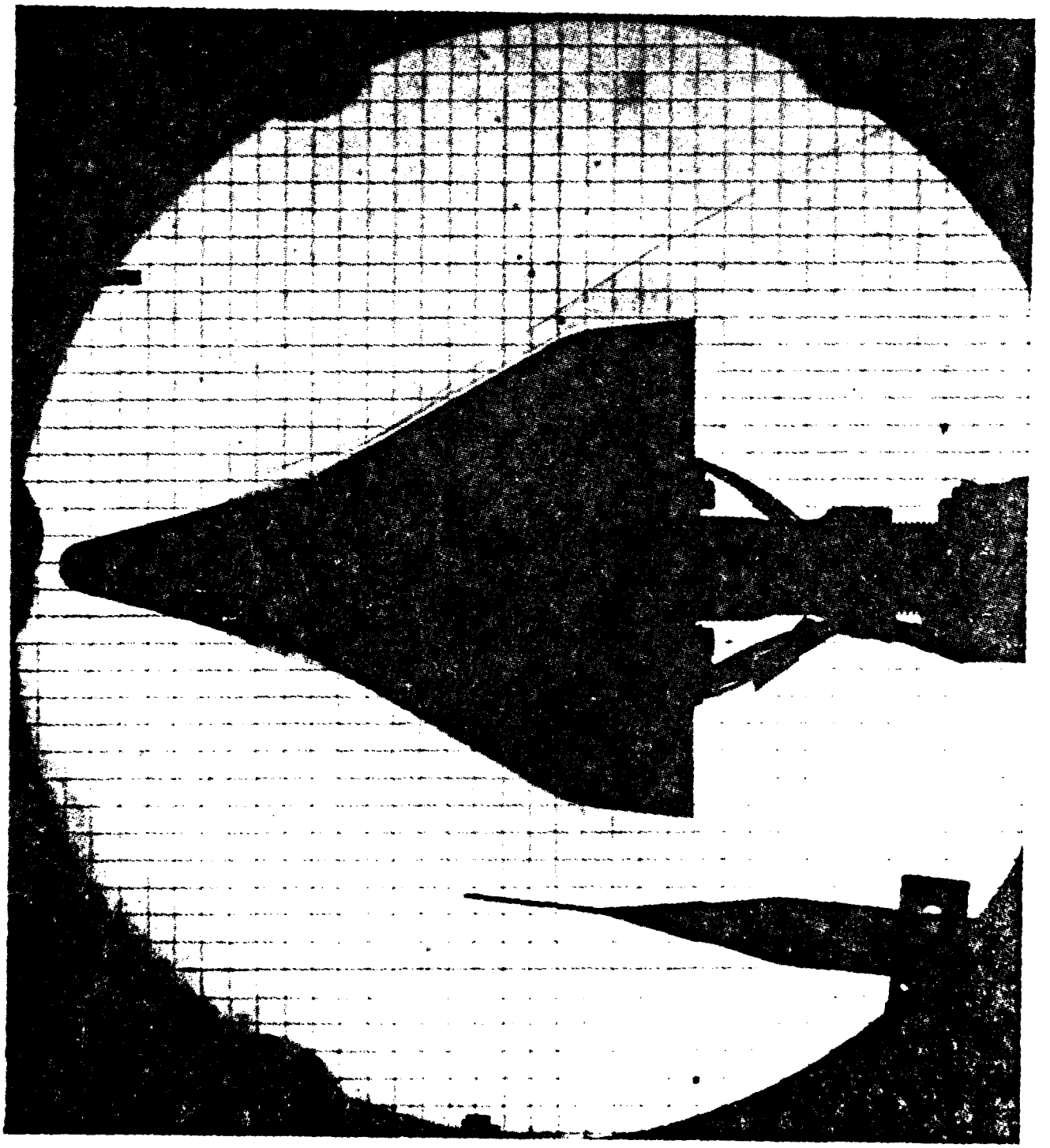

FIGURE 4

Schlieren Flow Field
Run No. 610 - Model N
$M_\infty = 20$, $Re_\infty = 3.0 \times 10^6/ft$, $\alpha = 0^\circ$

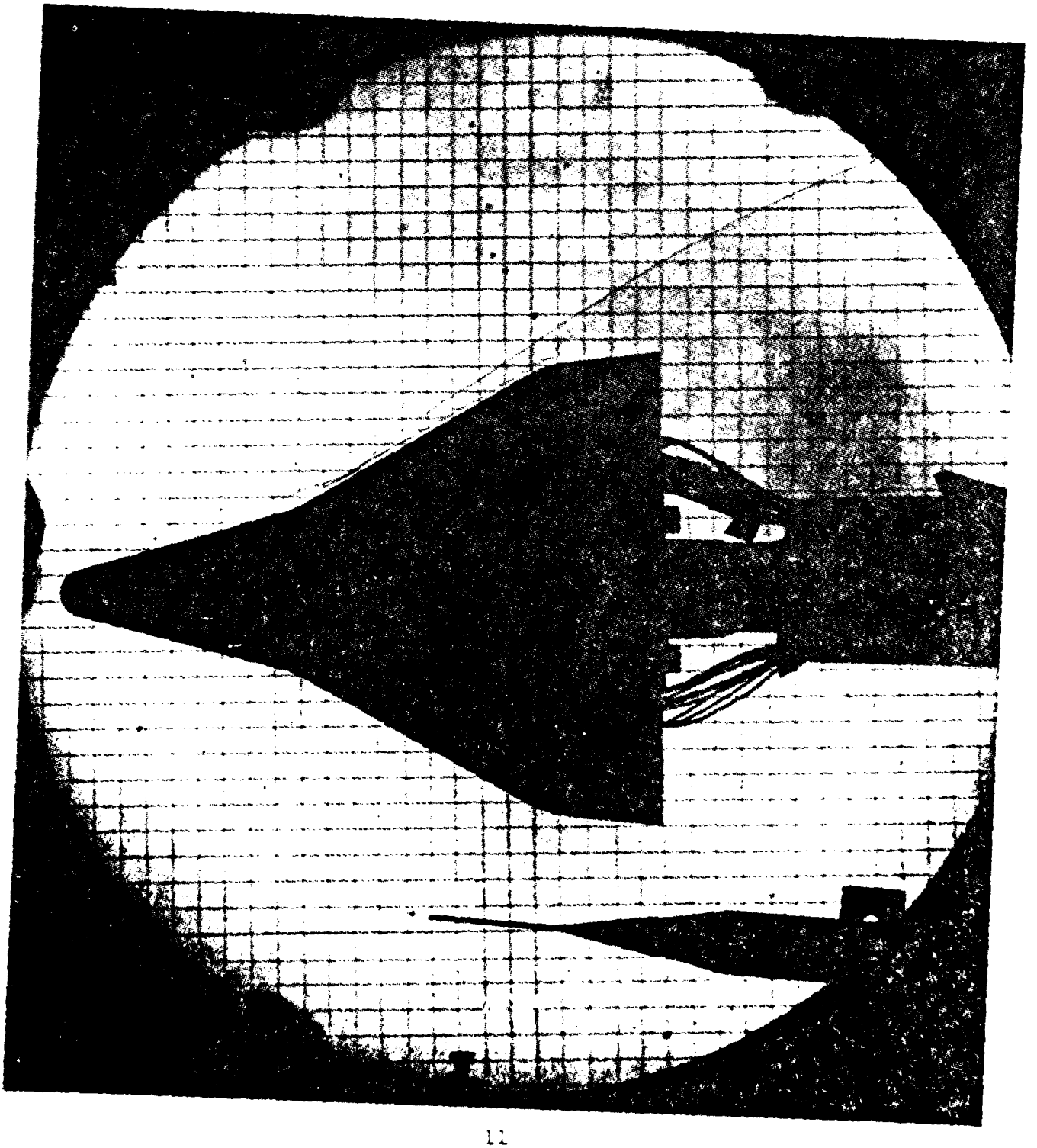

FIGURE 5

Schlieren Flow Field
Run No. 611 - Model N
$M_{\infty} = 16$, $R_{e_{\infty}} = 4.5 \times 10^6/ft$, $\alpha = 0^{\circ}$

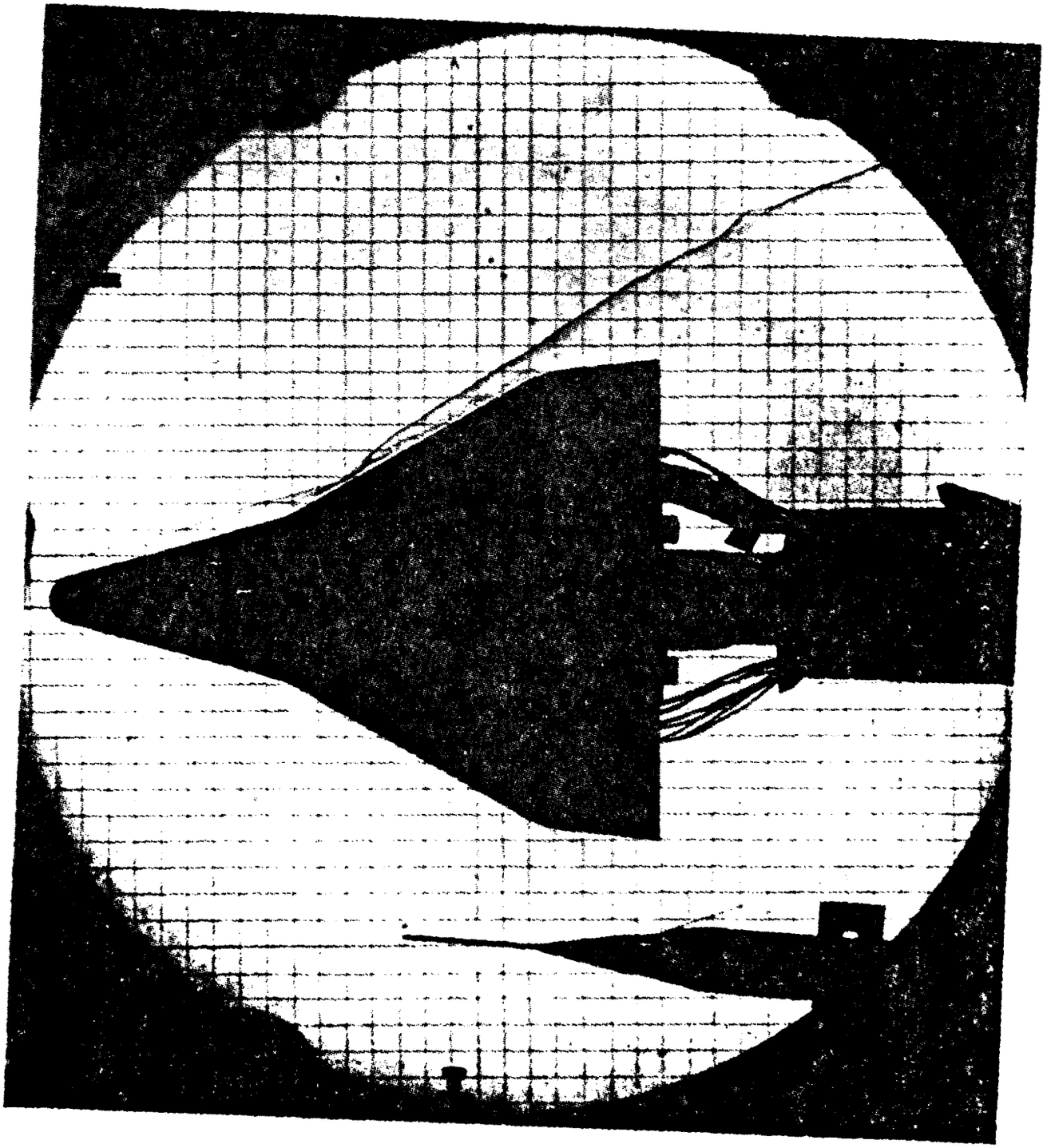

FIGURE 6

Schlieren Flow Field
Run No. 612 - Model N
$M_\infty = 16$, $Re_\infty = 9 \times 10^6/ft$, $\alpha = 0^\circ$

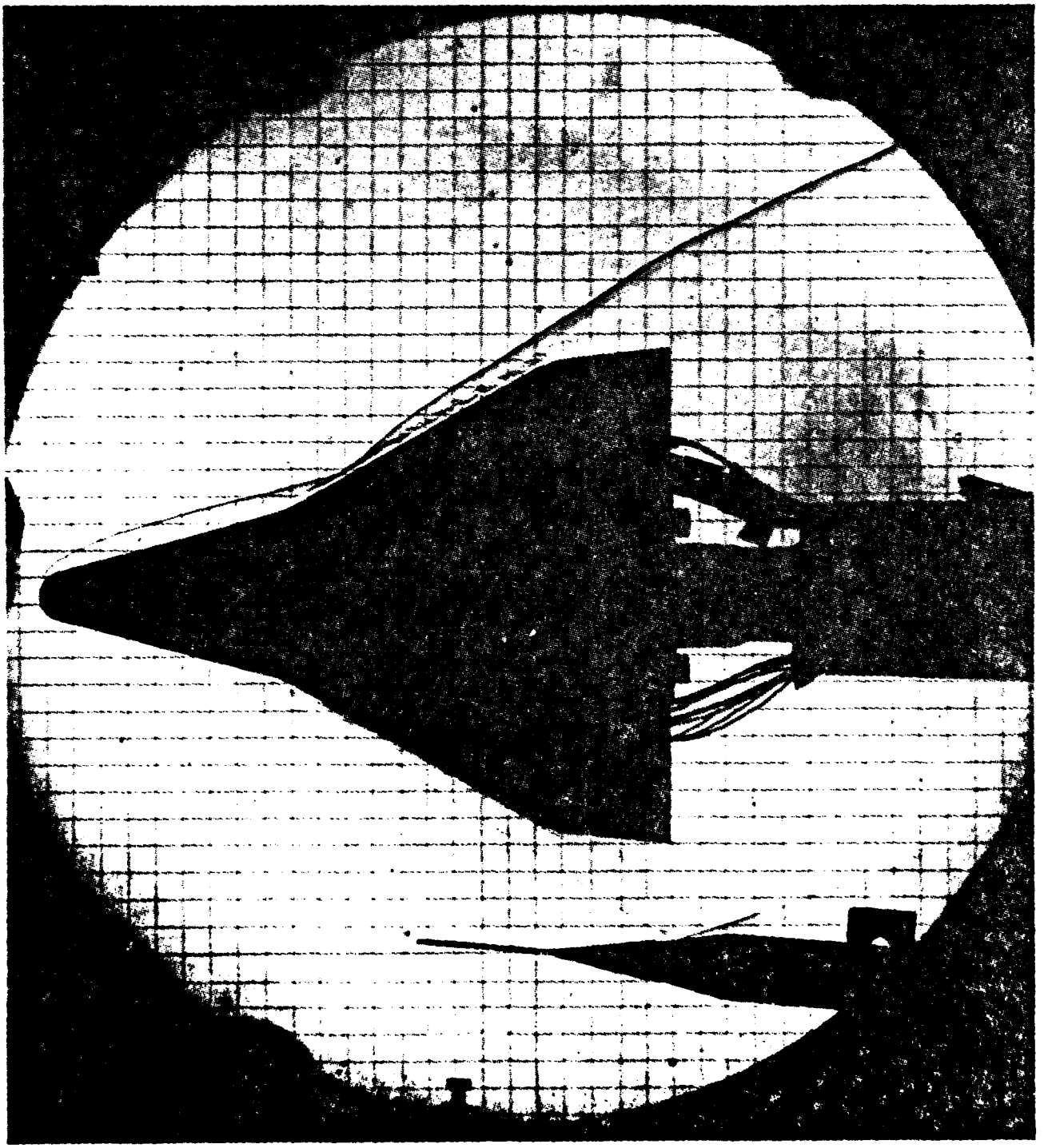

FIGURE 7

Schlieren Flow Field
Run No. 616 - Model N
$M_\infty = 20$, $Re_\infty = 3 \times 10^6/ft$, $\alpha = +5^\circ$

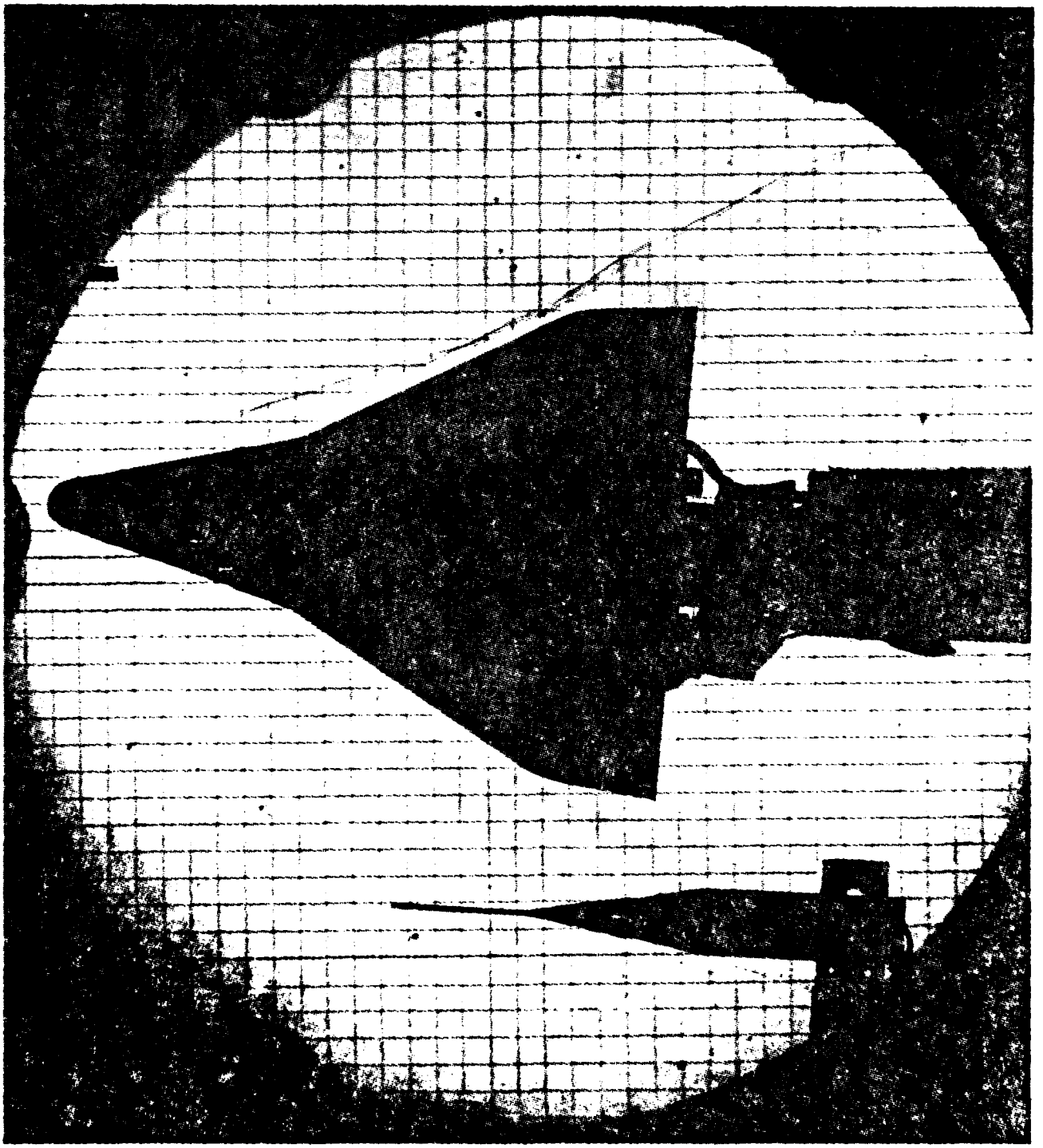

FIGURE 8

Schlieren Flow Field
Run No. 615 - Model N
$M_\infty = 20$, $Re_\infty = 3 \times 10^6/ft$, $\alpha = -5^\circ$

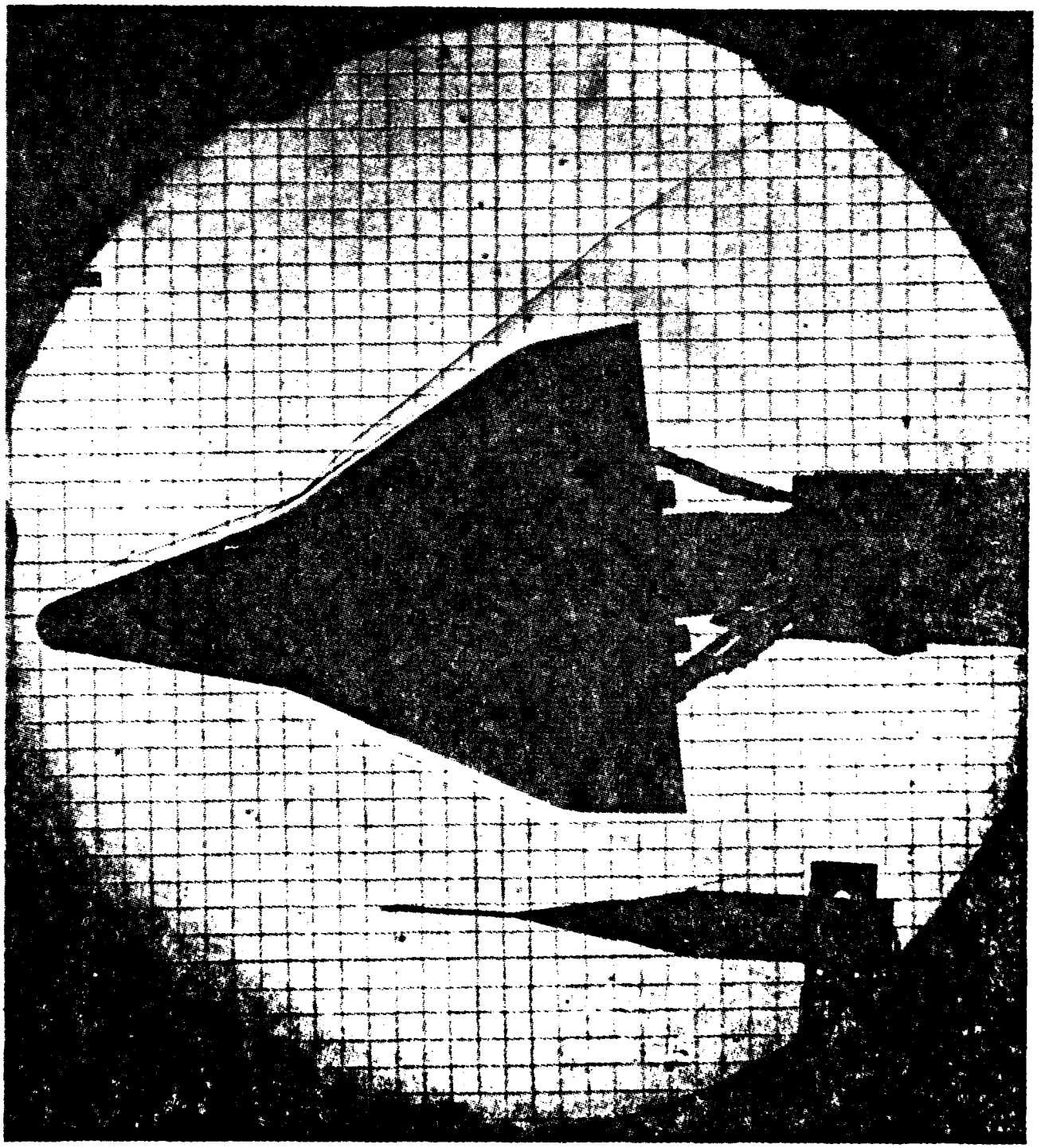

FIGURE 9

Schlieren Flow Field
Run No. 614 - Model N
$M_\infty = 16$, $Re_\infty = 9 \times 10^6/ft$, $\alpha = -5^\circ$

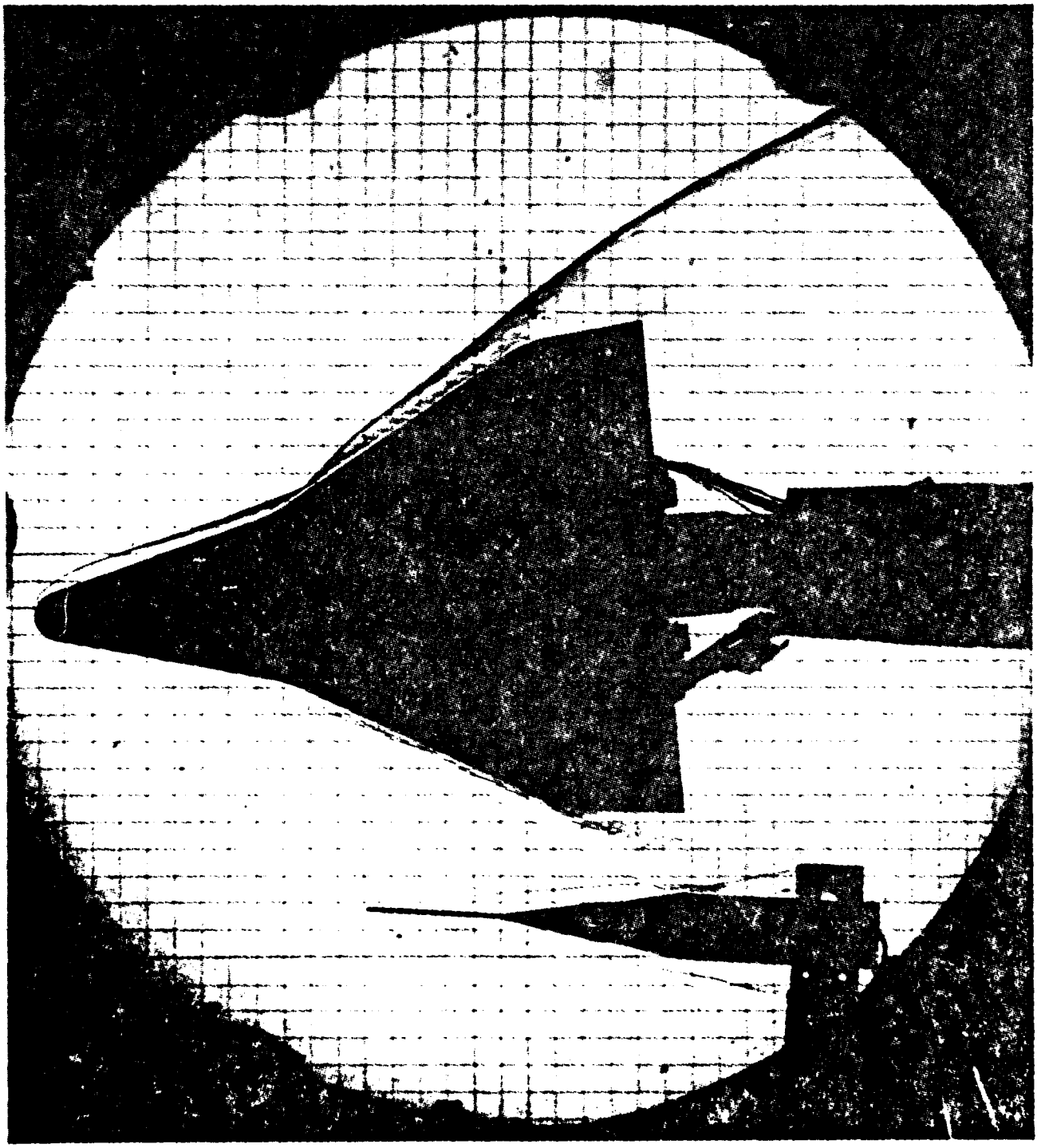

FIGURE 10

Schlieren Flow Field
Run No. 624 - Model N
M_{∞} = 16, $R_{e\infty}$ = 2 x 10^6/ft, α = +20°

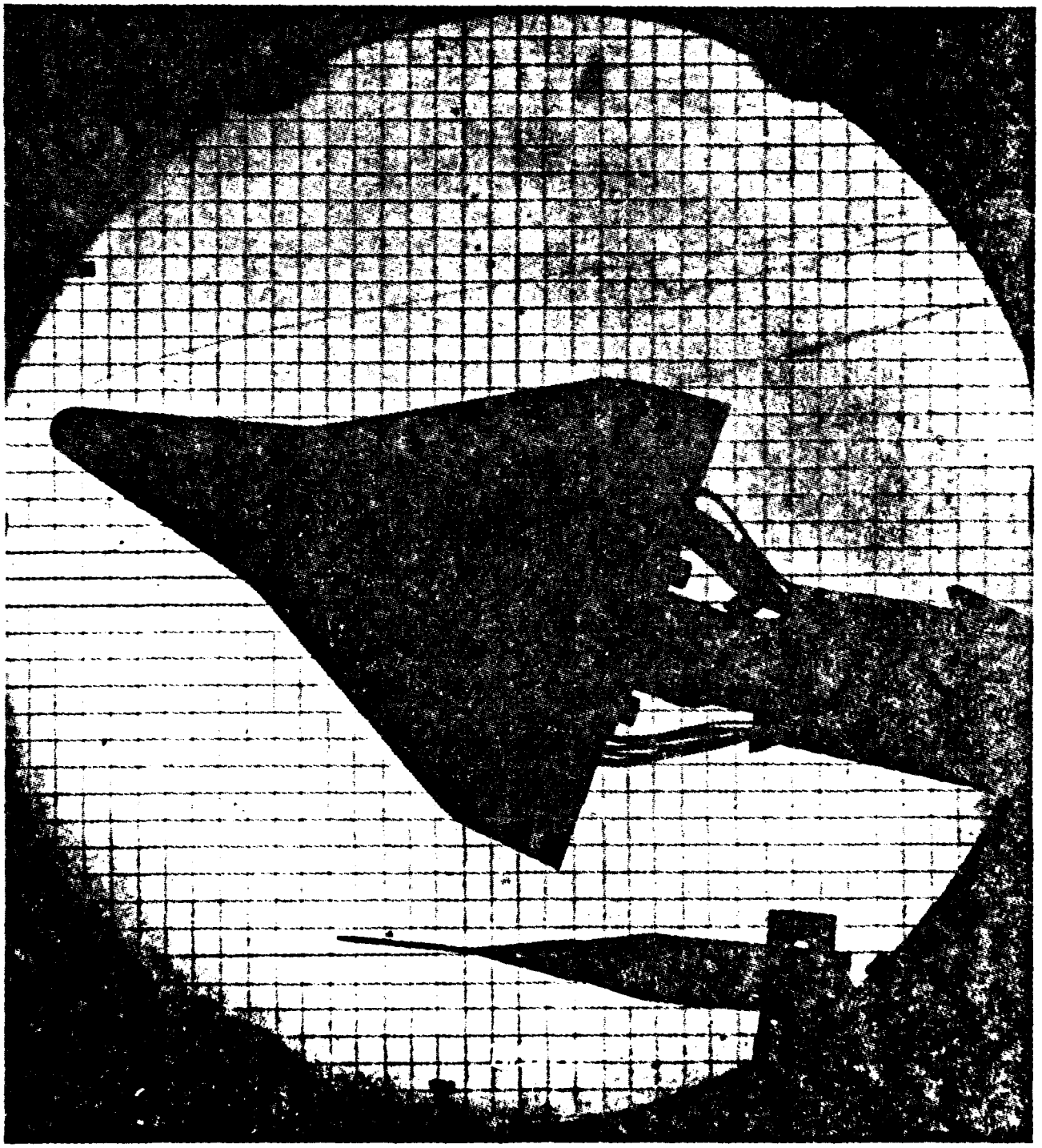

FIGURE 11

Schlieren Flow Field
Run No. 623 - Model N
$M_\infty = 20$, $Re_{\infty/ft} = 3.3 \times 10^6$/ft, $\alpha = +20^\circ$

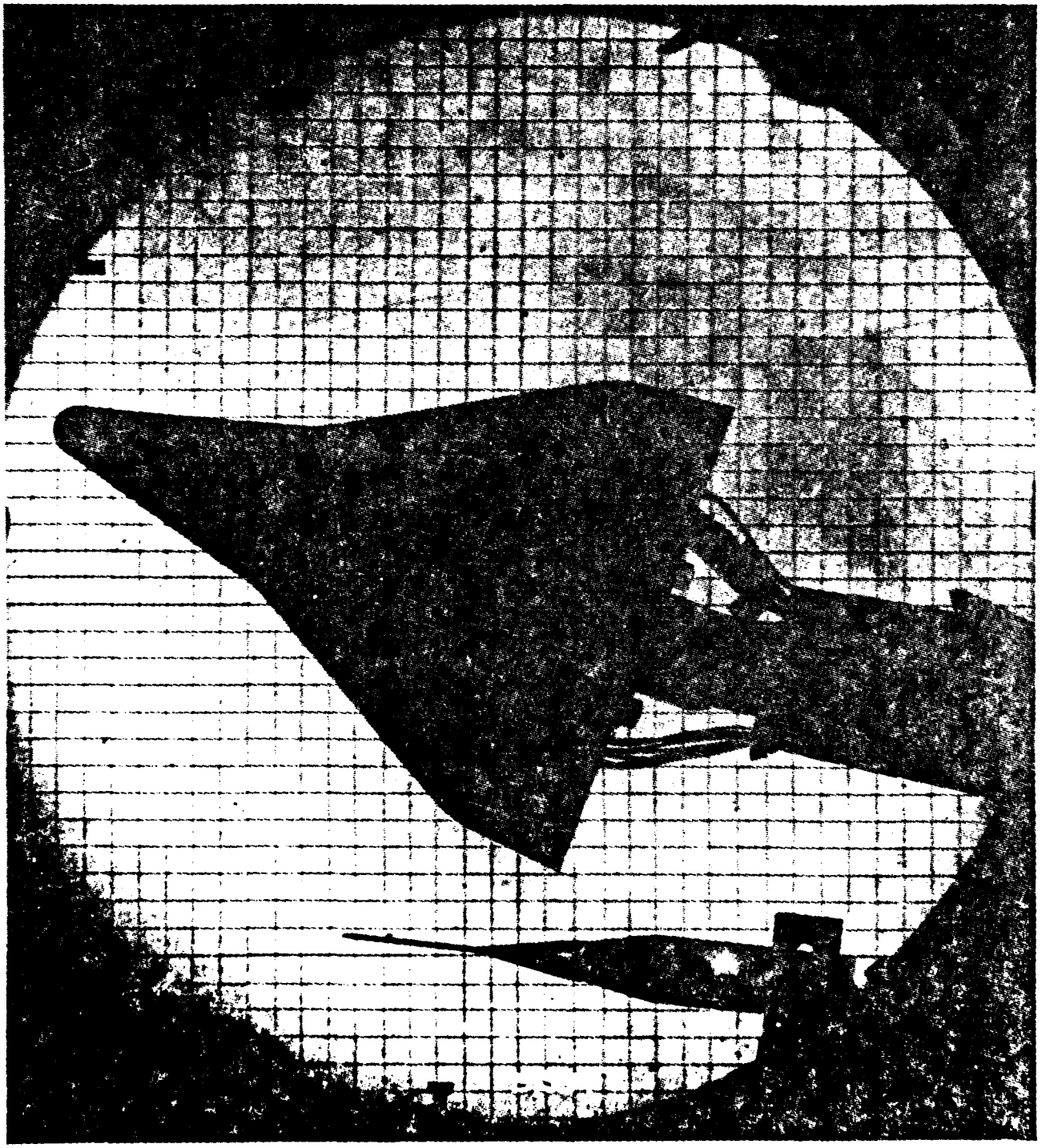

FIGURE 12

Schlieren Flow Field
Run No. 819 - Model N
$M_\infty = 16$, $Re_\infty = 4.5 \times 10^6$, $\alpha = +20^\circ$

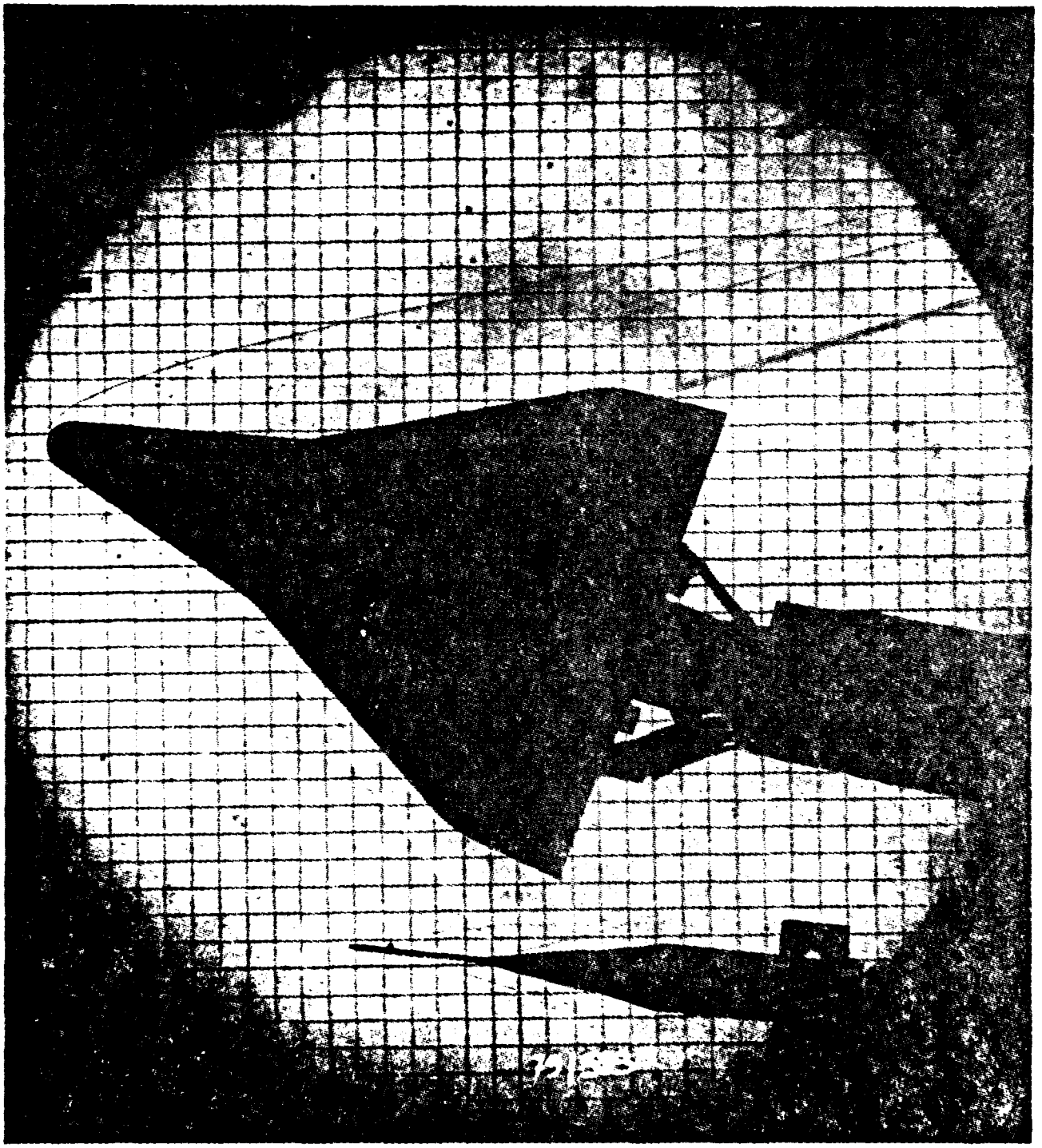

FIGURE 13

Schlieren Flow Field
Run No. 620 - Model X
$M_\infty = 16$, $R_{e_\infty} = 3 \times 10^6$/ft, $\alpha = +20^\circ$

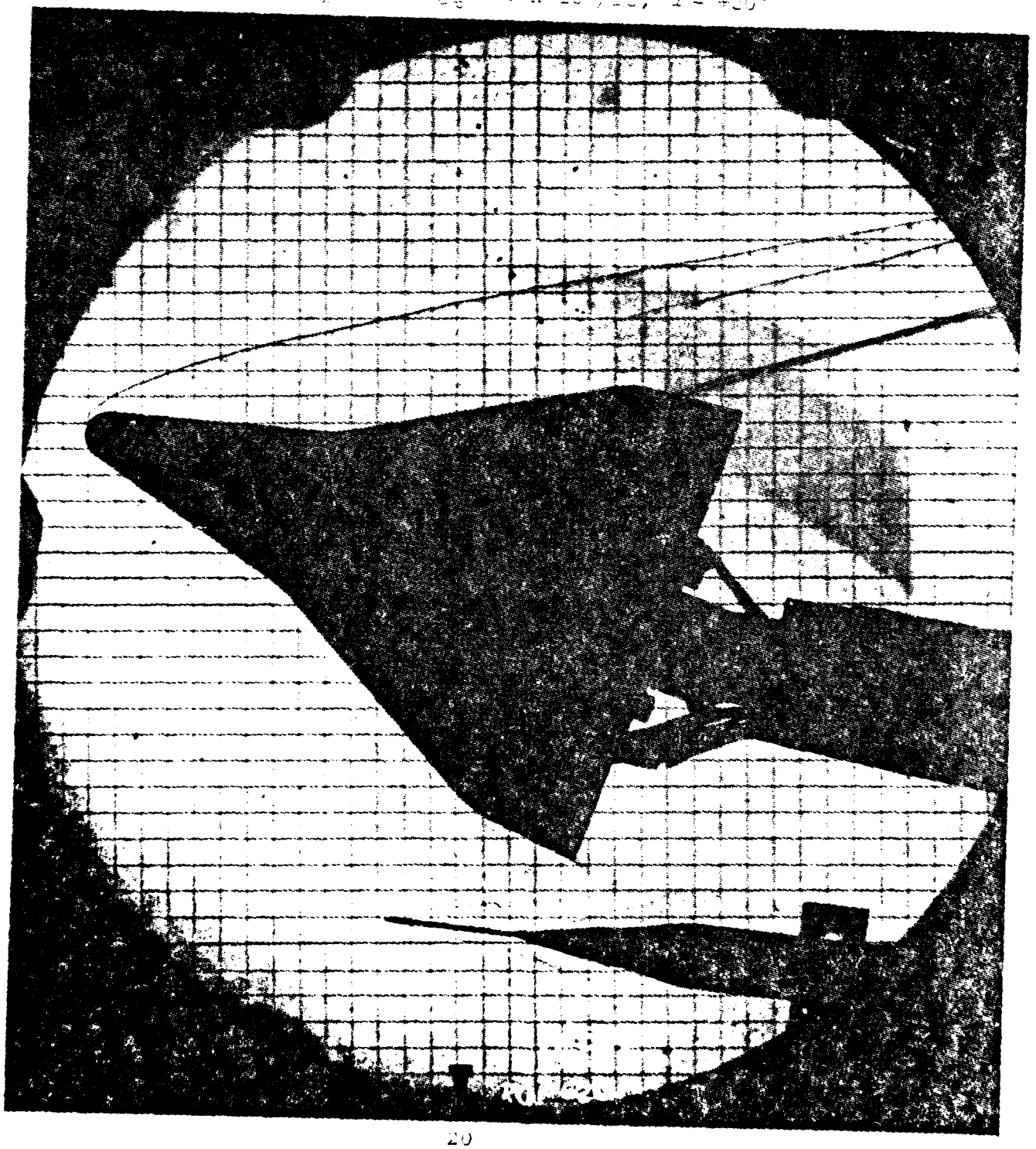

END

DATE
FILMED

4-80

DTIC